Semiclassical theory of the eigenvalues of a prolate cavity via the adiabatic switching method

1993 J. Phys. A: Math. Gen. 26 4749

(http://iopscience.iop.org/0305-4470/26/18/035)

J. Phys. A: Math. Gen. 26 (1993) 4749–4765. Printed in the UK

Semiclassical theory of the eigenvalues of a prolate cavity via the adiabatic switching method

F Brut and R Arvieu

Institut des Sciences Nucléaires, F-38026 Grenoble Cédex, France

Received 13 July 1992, in final form 24 February 1993

Abstract. The eigenvalues of a prolate cavity (with axial symmetry) are studied as a function of the deformation for an ellipsoidal shape by using the adiabatic switching method (ASM). The method uses, as the only quantum mechanical ingredients, trajectories which obey the Einstein–Brillouin–Keller (EBK) rules in the spherical case. The cavity is then adiabatically deformed and the energy change results from work done by the force exerted by the cavity on the particle. The resulting spectrum is in excellent agreement with the exact spectrum as well as with the semiclassical one calculated by the EBK method. The crossing of a separatrix for $L_z = 0$ (L_z is the z-component of the orbital angular momentum) does not affect our results significantly. The method is used to calculate the total energy of a system of independent nucleons as a function of deformation. Comparison with the Balian–Bloch formula shows that the ASM is producing correctly shell effects which are absent in the formula.

1. Introduction

The occurrence of regular and chaotic trajectories in bound systems with many degrees of freedom has renewed the interest for semiclassical methods. Indeed, these methods link classical and quantum mechanics and also provide some cheaper tools in order to find the highly excited energy spectra, even when the exact quantum calculation becomes very difficult to apply. In addition, semiclassical methods could give a deeper understanding of complicated systems owing to their classical origin. For bound Hamiltonian systems, most of the popular quantization procedures are based on the Einstein–Brillouin–Keller (EBK) [1] quantization method of phase-space tori. The problem with these approaches is to find the appropriate sets of initial conditions which correspond to some definite values for the actions of the system.

Among the variety of methods [2], the adiabatic switching method (ASM), deduced from the Ehrenfest adiabatic hypothesis [3], was first proposed by Solov'ev [4] who has studied a two-dimensional anharmonic oscillator perturbed by cubic terms on coordinates. The basic idea was very simple: under slow changes of the parameters of the system, certain quantities remain approximately constant, they turn out to be the classical actions. Practical use of ASM is thus very clear: if for a set of given values for the parameters of the system it is possible to satisfy the EBK quantization conditions, then the actions remain close to their initial values when these parameters are slowly varying while, at the same time, the trajectory is slowly changing. In principle, the validity of the adiabatic theorem in classical mechanics has been proven rigorously only for one-dimensional Hamiltonians. Nevertheless, the ASM has been extensively applied to various N-dimensional Hamiltonian systems, the phase space of which showed regular and chaotic regions [4–26]. However, application of the ASM requires

0305-4470/93/184749+17$07.50

in principle that two conditions are fulfilled: the classical tori in phase space must exist during the switching procedure and the switching time must be greater than any intrinsic period of the motion. Even though the first condition is not realized, the ASM has been extended with success to the quantization of mildly chaotic classical systems [6, 10, 11, 13, 14, 19, 24]. The latter condition does not allow change of the topology of the trajectory during switching and thus crossing a separatrix. In previous works [4-26], the energies obtained by using the ASM were found to be in very good agreement with those obtained by exact semiclassical calculations, or by solving the Schrödinger equation. It was shown also that randomly chosen initial conditions could remove the oscillations on the energy due to the finite value of the switching time. In a previous publication [8] on the single particle energies of a nuclear potential with spherical symmetry, we have also successfully used the ASM in order to calculate the energy levels as a function of the mass number from $A=208$ (Pb) to $A=16$ (O). The slowly varying parameter was the range of the potential. Obviously, the system was one-dimensional and we easily verified the validity of the ASM, for any intermediate value of the mass number, either by calculating the exact semiclassical solution or by comparison with the quantum eigenvalue. In the studies of two-dimensional systems quoted above, the invariance of the actions was most often postulated but not verified during the adiabatic switching. A small classical mechanical energy variance at the end of the switching was employed to measure the degree of convergence of the ASM calculation.

The aim of this paper is to use the ASM in a simple but non-trivial example: we will follow the eigenvalues of a prolate cavity with axial symmetry as a function of its deformation. This example is of interest because it is possible to calculate the intrinsic frequencies and the actions at each step and to analyse their variations in time. This system presents the property to be two-dimensional and integrable, therefore the variation of the actions during the adiabatic switching can be studied in a detailed way [27]. Its phase space is known [18] to be organized differently according to the value of the projection L_z of the angular momentum on the symmetry axis. If $L_z \neq 0$ the trajectories correspond to a unique topology while there are two topologies for $L_z=0$. Therefore, for $L_z=0$ all the semiclassical eigenstates cross the separatrix for a value of the deformation which is exactly known [18]. The influence of these crossings on the validity of the method can be studied in the same manner. On the other hand, a prolate cavity is a simplified example of a deformed nuclear potential. Of course, the energy levels of a deformed nuclei have been studied for many years [28]. It is not so well known that most of their variation with deformation has a classical origin which can be revealed by using the ASM. In some of our previous work [8, 18, 29, 30], we have already studied the phase space structure of nuclear single particle potentials. This paper concentrates on a simplified version from which much can be learned. In particular, we study the total energy as a function of deformation of a system of nucleons in the cavity using the ASM. In this way shell effects occur and our result can be compared with the asymptotic formula of Balian and Bloch [31], well known in nuclear physics [32].

2. Outline of the method

The adiabatic switching method is clearly explained elsewhere for non-integrable Hamiltonian systems [22, 24]. It has been developed to find semiclassical energy spectra

of non-integrable Hamiltonians as a function of internal parameters, such as the magnetic field. Let us just recall that the general principle is to start with a zero-order Hamiltonian which is integrable, the semiclassical energies of which are easy to find. The change in the energy levels that result originates from the classical work done on the particle during its motion. The aim of the method is to calculate such changes which lead to splitting, crossing of levels and, as we shall see, to shell effects. Of course these changes are also present in the EBK method but their physical origin is totally unpredictable. These energies are indeed obtained by searching the invariant tori in phase space which are labelled by the semiclassical actions which fulfil the EBK quantization conditions. Then, an adiabatic change on this initial Hamiltonian is made in order to reach, at the end of the switching, the required non-integrable Hamiltonian. Starting on a semiclassical torus of the zero-order Hamiltonian, the classical actions are conserved during adiabatic switching and labelled at any time the semiclassical tori. Obviously, these tori must exist throughout switching. Nevertheless some previous works [19, 24] have used the method for systems for which chaos exists but is not well developed in phase space. In a prolate cavity, as the motion of a free particle is always separable in suitable coordinates, there are only regular trajectories. Thus, in such a system, we would study the validity of the ASM in a non-trivial case without introducing other phenomenon like chaotic motion. The adiabatic condition implies that the switching time must be greater than any intrinsic periods of the system. Thus we are expecting that the method will fail if the topology of semiclassical trajectories is changing during the switching. More precisely, this means that passing through a separatrix, for which one intrinsic period of the motion becomes infinite, must in principle lead to the failure of the ASM. If, during the switching, two frequencies of the motion become rationally related—a resonance region—it has been shown [22] that some of these primary resonance crossings are equivalent to separatrix crossings, even if the topology of the trajectory is not changed by the resonance. Therefore, resonance regions will induce some failure of the ASM, and this point will be clearly underlined by following the values of the actions as a function of the switching time [27].

Motion of a free particle inside a prolate cavity is separable in spheroidal prolate coordinates:

$$\begin{aligned} x &= f \sinh \varepsilon \sin \xi \cos \phi \qquad 0 \leqslant \phi \leqslant 2\pi \\ y &= f \sinh \varepsilon \sin \xi \sin \phi \qquad 0 \leqslant \varepsilon \leqslant \infty \\ z &= f \cosh \varepsilon \cos \xi \qquad 0 \leqslant \xi \leqslant \pi \end{aligned} \tag{1}$$

where the z axis is the symmetry axis of the cavity and $2f$ is its focal distance:

$$f^2 = a^2 - b^2 \tag{2}$$

a and b, the larger and smaller semiaxis, respectively, are related by the volume conservation condition, a condition which is traditional in nuclear physics:

$$ab^2 = R_0^3 = \text{constant} \tag{3}$$

R_0 is the radius of a sphere having the same volume. The deformation parameter is

$$\mu = \frac{a}{b}. \tag{4}$$

The equations of motion [32] give the canonical momenta p_ε and p_ξ as a function of ε and ξ respectively, and also of $p_\phi = L_z$ as well as the energy E and of a separation

constant C. The energy E of the particle is written as

$$E=\frac{\hbar^2k^2}{2m} \tag{5}$$

and the momenta are given by

$$p_\varepsilon^2=k^2f^2\cosh^2\varepsilon-\frac{L_z^2}{\sinh^2\varepsilon}-C \tag{6a}$$

and

$$p_\xi^2=C-k^2f^2\cos^2\xi-\frac{L_z^2}{\sin^2\xi} \tag{6b}$$

where the separation constant C must be expressed in terms of the scalar product of the two angular momenta with respect to each focus [18] as

$$C=l_1\cdot l_2+k^2f^2. \tag{6c}$$

(Note: there is a misprint in equation (10) of [18] in which the k^2f^2 term is missing.)

Inside a prolate cavity, a generic trajectory with $L_z\neq 0$ never crosses the z axis and is represented in figure 1 in cylindrical coordinates on a plane (ρ, z). In 3D configuration space, a trajectory is obviously built by segments of straight lines limited by the bounces on the boundary. On the plane (ρ, z), this trajectory is made by segments of hyperbolas (see figure 1). When one canonical momentum, p_ε or p_ξ, becomes zero, the particle is on one of the two caustics. The first caustic is an ellipsoid homofocal to the boundary, and corresponds to $p_\varepsilon=0$; the track of this caustic is the dotted line in figure 1. The second one is a two-sheets hyperboloid, also homofocal to the boundary, corresponding to $p_\xi=0$; its tracks on the trajectory plane (ρ, z) is represented in figure 1 by dashed lines. These two caustics are consequences of the centrifugal barrier, as L_z is finite

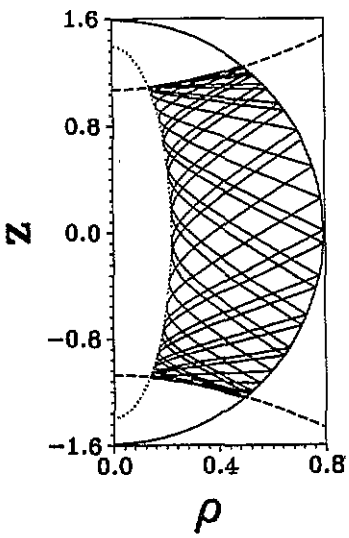

Figure 1. Generic $L_z\neq 0$ trajectory in a prolate cavity with a 2:1 shape. The trajectory is represented in cylindrical coordinates (ρ, z). The two dashed lines are the footsteps of the two sheets hyperboloidal caustic and the dotted line is the track of the ellipsoidal caustic.

and non-zero, as was discussed by Arvieu *et al* [18]. For the trajectory shown in figure 1, the coordinate ε varies between the two values ε_0 defined by the ellipsoidal caustic and ε_1 corresponding to the boundary. The angle ξ could take any value between ξ_0 defined by the symmetry axis and the upper sheet of the hyperboloidal caustic, and $\pi-\xi_0$ corresponding to the angle between the z axis and the lower sheet of the hyperboloidal caustic.

For the $L_z=0$ trajectories, one of the two preceding caustics disappears and merges in the symmetry axis. Thus two general topologies for the trajectories exist and are shown in figure 2. The trajectory is now represented in a meridian plane (x, z) and thus could present an elliptical caustic or an hyperbolic caustic depending on the sign of $l_1 \cdot l_2$ [18]. For $L_z=0$, the semiclassical energy levels could cross the separatrix between the two topologies and it is our purpose to see the applicability of the adiabatic switching method in the neighbourhood of the crossing.

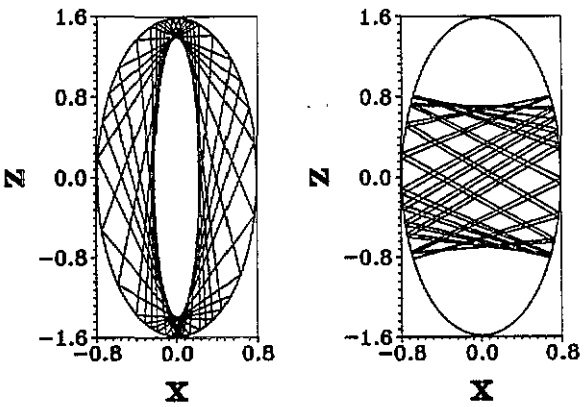

Figure 2. Generic $L_z=0$ trajectories in a prolate cavity with a 2:1 shape. Left: trajectory with an elliptical caustic. Right: trajectory with a hyperbolic caustic.

Semiclassical quantization in a prolate cavity requires finding an initial condition which fulfils the EBK quantization conditions [1] for each set of quantum numbers (nlm) [18]:

$$I_\varepsilon = \frac{1}{\pi}\int_{\varepsilon_1}^{\varepsilon_0} p_\varepsilon \, \mathrm{d}\varepsilon = (n+\tfrac{3}{4})\hbar \tag{7a}$$

$$I_\xi = \frac{1}{\pi}\int_{\pi-\xi_0}^{\xi_0} p_\xi \, \mathrm{d}\xi = (l-|m|+\tfrac{1}{2})\hbar \tag{7b}$$

$$I_\phi = L_z = m\hbar \tag{7c}$$

if we take the 'primitive' approximation and not a uniform quantization condition (see discussion in [18], [33] and [34] for more details). Obviously the two classical actions I_ε and I_ξ defined by (7) are function of the energy E and of the separation constant C, via the two canonical momenta p_ε and p_ξ defined by (6). Solving the semiclassical quantization for a given set (nlm) of quantum numbers consists of finding an initial condition or the energy and the separation constant which satisfies (7). This task, which will be done later, can be avoided if we are interested in a great number of single-particle energy levels. We can use instead the ASM.

Starting with a sphere of radius R_0, it is easy to find an initial condition on a semiclassical torus corresponding to the quantum numbers (nlm) [8, 35]. Then, the sphere is adiabatically deformed to a prolate ellipsoidal shape, by holding the volume constant and by setting deformation time dependent

$$\mu(t)=\frac{a(t)}{b(t)}=1+\lambda(t) \tag{8}$$

where $\lambda(t)$ is the switching function which satisfies $\lambda(0)=0$ and $\lambda(T)=1$, where T is the switching time. The analytical form of the switching function was extensively studied by Johnson [7] and the most commonly used is

$$\lambda(t)=\frac{t}{T}-\frac{\sin 2\pi t/T}{2\pi}. \tag{9}$$

Now, the boundary equation of the prolate cavity becomes time dependent and the semiaxes are expressed as

$$a(t)=R_0[\mu(t)]^{2/3} \tag{10a}$$

$$b(t)=R_0[\mu(t)]^{-1/3}. \tag{10b}$$

Let us assume that the particle is starting, at time t_0, on a point $M_0(x_0, y_0, z_0)$ located on the boundary of the cavity. The velocity of the particle is then v_0. The problem is now to find the time-of-flight t of the particle until it again hits the boundary at a point $M_1(x_1, y_1, z_1)$, the coordinates of which are given by the equations of motion and by the equation of the boundary:

$$\boldsymbol{OM}_1=\boldsymbol{OM}_0+\boldsymbol{v}_0\cdot t \tag{11}$$

$$\frac{x_1^2+y_1^2}{b^2}+\frac{z_1^2}{a^2}=1 \tag{12}$$

where the semiaxes a and b are time dependent and are defined by equations (8) and (10). When the time-of-flight t is numerically determined, the perfect reflexion laws in M_1 are written for the particle bouncing on the cavity wall. Let $\boldsymbol{n}_1$ be the unit normal vector to the boundary in M_1; then, if the velocities of the particle before and after the bounce in M_1 are $\boldsymbol{v}_i$ and $\boldsymbol{v}_f$, respectively, we have:

$$(\boldsymbol{v}_i-\boldsymbol{v}_f)\wedge\boldsymbol{n}_1=0 \tag{13a}$$

$$(\boldsymbol{v}_i+\boldsymbol{v}_f-2\boldsymbol{u}_1)\cdot\boldsymbol{n}_1=0 \tag{13b}$$

where $\boldsymbol{u}_1$ is the velocity of the boundary in M_1. In the particular case of a prolate cavity, we could define $\boldsymbol{u}_1$ by the scalar product

$$\boldsymbol{u}_1\cdot\boldsymbol{n}_1=\left\{\frac{x_1^2+y_1^2}{b^2}\frac{\dot{b}}{b}+\frac{z_1^2}{a^2}\frac{\dot{a}}{a}\right\}\Big/Q \tag{14}$$

with

$$Q=\left\{\frac{x_1^2+y_1^2}{b^4}+\frac{z_1^2}{a^4}\right\}^{1/2} \tag{15}$$

and

$$\frac{\dot{a}}{a}=\frac{1}{a}\frac{\mathrm{d}a}{\mathrm{d}t}\bigg|_{t_0+t}=\left[\frac{2}{3\mu}\frac{\mathrm{d}\mu}{\mathrm{d}t}\right]_{t_0+t} \tag{16a}$$

$$\frac{\dot{b}}{b}=\frac{1}{b}\frac{\mathrm{d}b}{\mathrm{d}t}\bigg|_{t_0+t}=\left[-\frac{1}{3\mu}\frac{\mathrm{d}\mu}{\mathrm{d}t}\right]_{t_0+t} \tag{16b}$$

where $\mu(t)$ is defined by (8). Obviously, when the particle is flying between M_0 and M_1, its energy remains constant. When it hits the boundary, its energy could suddenly increase or decrease by steps depending on the sign of the scalar product in (14).

This method is applied to every semiclassical level in a prolate cavity. Starting with an initial condition on the semiclassical tori of the spherical cavity, the adiabatic switching ends when the deformation μ in the prolate cavity reaches the value 2. The semiclassical energy levels can thus be followed during the switching procedure and the energies are drawn as a function of the deformation μ. Comparison of the results obtained by using the ASM, on one hand, and quantum calculations as well as exact semiclassical quantization, on the other hand, is presented in the next section.

3. Results

The validity of the adiabatic approximation requires that the switching time T tends to infinity. The initial set of classical actions, which are defined for a spherical cavity, tag, in principle, the semiclassical levels of the deformed cavity during the switching procedure. However, in practical calculations, T is always finite, and thus the final energy obtained depends not only on the initial semiclassical actions, but also on the initial angles which are the conjugate variables of the actions. These angles are determined by the exact position of the initial condition on the surface of the starting semiclassical torus. In other words, the particle energy will be not only a function of the deformation and of the set of initial semiclassical actions, but also a function of these conjugate angles during the adiabatic switching. As the initial conditions are periodic in these angles, with a period of 2π, the energy dependence on the angles could be removed by averaging the energies obtained for each value of the deformation, by starting from different randomly chosen initial conditions laying on the same semiclassical torus. The averaging procedure should cancel the oscillating part of the semiclassical energies as was discussed by Skodje *et al* [6] and by Johnson [7]. Examples of such behaviours are shown in figure 3 for the particular $L_z=1$ level starting from the $1g$ spherical multiplet. The energy of this level is obtained by an average over 25 different initial conditions chosen at random; the value of the energy is given by $(kR_0)^2$ where k and R_0 are defined by equations (3) and (5). To emphasize the oscillation in figure 3, the preceding mean energy is subtracted from the energy obtained from only one initial condition at each value of the deformation. In figure 3(a) the switching time T is relatively short to emphasize the amplitudes of the oscillations in each of these two different initial conditions. When the number of bounces of the particle on the cavity is increased, which is simply done by increasing the time T, the oscillation amplitudes δE decrease as shown in figure 3(b). This behaviour is generic for the energy during the switching and does not depend on any particular choice of the initial quantum numbers. These oscillation phenomena are present also when other dynamic quantities, such as the classical actions, are calculated during switching [27].

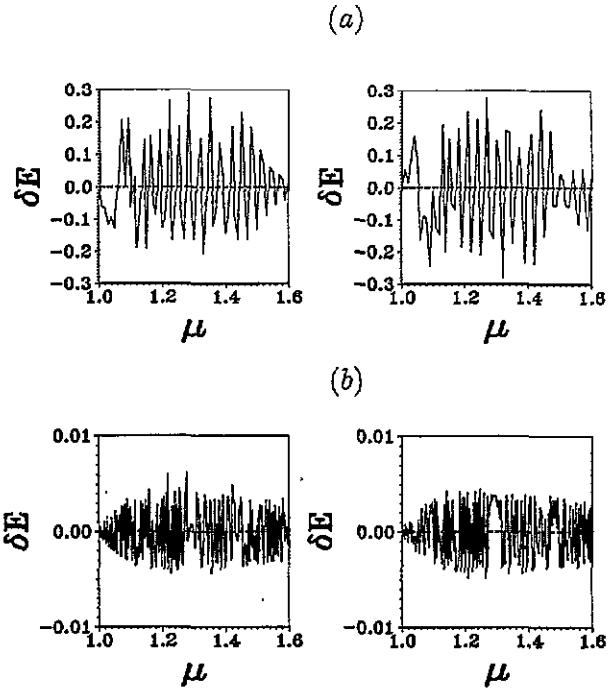

Figure 3. Deviations from the average energy for some particular initial condition. The time evolution of the energy deviation of the $L_z = 1$ level issued from the $1g$ spherical multiplet is drawn during adiabatic switching. Frames (a) correspond to two different initial conditions for only 140 bounces of the particle on the boundary during the switching time. Frames (b) correspond to 9200 bounces of the particle on the boundary. Notice the change of the vertical scale between (a) and (b).

Results are presented in table 1 for some of the low-lying states in the prolate cavity as a function of the deformation μ. The method used to obtain the quantum spectrum in a prolate cavity was extensively discussed in [18] and [33]. The semiclassical energies E_{SC} are calculated using the semiclassical quantization conditions given by (7). For this purpose, for a given set of quantum numbers (nlm) and for each value of the deformation μ, a semiclassical energy E_{SC} and a separation constant C must be found in order to fulfil simultaneously the semiclassical quantization rules. For each value of the deformation, the adiabatic switching energy E_{ASM} is the result of the average over 25 particle energies obtained by running trajectories starting on the same semiclassical torus. For the prolate cavity, it is also possible [27] to calculate the classical actions of the particle, their averaged values $\bar{I}_\varepsilon$ and $\bar{I}_\xi$ are shown in table 1 and must be compared to their initial values—for $\mu = 0$—which should be exactly invariant during the switching. The comparison with the initial values is a delightful proof of the validity of the ASM in this problem. The switching time function given by (9) is used with the same switching time T_f for all the energy levels reported in table 1. Of course, the number of bounces of the particle inside the cavity during switching increases with the energy of the particle. First, we must note that the adiabatically switched energy E_{ASM} is in excellent agreement with the exact semiclassical energy E_{SC}. Second, the relative deviation between the semiclassical E_{SC} and the exact quantum calculations E_Q, which is given by the sixth column in table 1, is of the same order

Table 1. Energy eigenvalues for some levels in a prolate cavity as a function of the deformation.

(n, l, m)	m	E_Q [a]	E_{SC} [b]	E_{ASM} [c]	ΔE [d]	$\bar{I}_z$ [e]	$\bar{I}_\xi$ [e]	Number of hits[f]
(1, 5, 0)	1.0	87.3512	86.8567	86.8567	6×10^{-3}	0.750 00	5.500 00	
	1.1	84.2153	83.6760	83.6754	6×10^{-3}	0.749 98	5.499 99	
	1.2	80.3945	80.0913	80.0898	4×10^{-3}	0.749 98	5.499 93	
	1.3	76.3135	76.2882	76.2864	3×10^{-4}	0.749 98	5.499 92	
	1.4	72.2796	72.3852	72.3828	1×10^{-3}	0.749 93	5.499 93	
	1.5	68.5193	68.4432	68.4412	1×10^{-3}	0.749 95	5.499 78	≈23 000
	1.6	65.1276	64.4308	64.4286	1×10^{-2}	0.750 02	5.499 59	
	1.7	62.1160	60.6274	60.6258	2×10^{-2}	0.750 00	5.499 81	
	1.8	59.4593	57.6566	57.6545	3×10^{-2}	0.750 14	5.499 46	
	1.9	57.1196	55.1910	55.1888	3×10^{-2}	0.750 15	5.499 48	
	2.0	55.0581	53.0987	53.0965	4×10^{-2}	0.750 19	5.499 49	
(1, 5, 2)	1.0	87.3512	86.8567	86.8567	6×10^{-3}	0.750 00	3.500 00	
	1.1	85.6854	85.0252	85.0248	8×10^{-3}	0.749 96	3.500 06	
	1.2	83.9727	83.2402	83.2394	9×10^{-3}	0.750 01	3.499 91	
	1.3	82.5621	81.7160	81.7157	1×10^{-2}	0.749 97	3.500 00	
	1.4	81.4788	80.5308	80.5304	1×10^{-2}	0.749 94	3.500 18	
	1.5	80.6940	79.6745	79.6749	1×10^{-2}	0.749 74	3.501 01	≈28 800
	1.6	80.1656	79.1026	79.1044	1×10^{-2}	0.749 73	3.501 07	
	1.7	79.8522	78.7656	78.7680	1×10^{-2}	0.749 76	3.500 92	
	1.8	79.7174	78.6200	78.6231	1×10^{-2}	0.749 76	3.500 95	
	1.9	79.7309	78.6300	78.6338	1×10^{-2}	0.749 75	3.501 01	
	2.0	79.8677	78.7671	78.7715	1×10^{-2}	0.749 75	3.501 01	
(1, 5, 5)	1.0	87.5312	86.8567	86.8567	6×10^{-3}	0.750 00	0.500 00	
	1.1	92.0019	91.1753	91.1760	9×10^{-3}	0.750 03	0.499 99	
	1.2	96.4252	95.5122	95.5133	9×10^{-3}	0.750 03	0.500 02	
	1.3	100.7908	99.8223	99.8235	1×10^{-2}	0.750 03	0.500 02	
	1.4	105.0938	104.0850	104.0862	1×10^{-2}	0.750 03	0.500 02	
	1.5	109.3327	108.2913	108.2924	1×10^{-2}	0.750 03	0.500 01	≈36 300
	1.6	113.5078	112.4378	112.4388	9×10^{-3}	0.750 03	0.500 02	
	1.7	117.6204	116.5239	116.5248	9×10^{-3}	0.750 02	0.500 02	
	1.8	121.6726	120.5505	120.5513	9×10^{-3}	0.750 02	0.500 01	
	1.9	125.6664	124.5194	124.5198	9×10^{-3}	0.750 01	0.500 02	
	2.0	129.6042	128.4324	128.4324	9×10^{-3}	0.750 00	0.500 01	

[a] Quantum-mechanical calculations [18, 33].
[b] Present results: exact semiclassical calculations using the quantization prescription given by equations (7).
[c] Present results: adiabatic switching method for an average over 25 different initial conditions.
[d] Relative deviation $\Delta E = |E_Q - E_{SC}|/E_Q$.
[e] Present results: the actions $\bar{I}_z$ and $\bar{I}_\xi$ are averaged over 25 different initial conditions for $m = 0$, and over only 10 for $m = 2$ or 5.
[f] *Approximate number of bounces of the particle during the full switching.*

of magnitude in a prolate cavity as it was in a spherical cavity. Third, it must be emphasized that the calculation of an eigenvalue using the exact semiclassical method is five to six times longer than the corresponding calculation using the ASM; quantum calculations [18, 30] require a computational time which is often longer than the exact semiclassical calculations, especially for high energy eigenvalues for which the basis truncature is a crucial problem.

The adiabatically switched energies for the $L_z = 0$ levels are of special interest due to the existence of a separatrix which is crossed often during switching. When the

shape of the cavity is adiabatically changed, the semiclassical trajectory begins with an elliptical topology (see figure 2(a)), then crosses the separatrix for a precise value of the deformation μ_{sep} [18], and afterwards ends with an hyperbolic topology (see figure 2(b)). In principle, the adiabatic hypothesis must fail for this particular value μ_{sep} as one of the intrinsic periods of the system tends to infinity. The results reported in table 1 concern only levels belonging to the $1h$ multiplet in the spherical cavity. For other multiplets, the same general features can be observed and the following conclusions are generic for a prolate cavity. For the $L_z = 0$ level shown in table 1, the separatrix crossing occurs for $\mu_{sep} = 1.6166$, and for deformations close to this value, the agreement between exact semiclassical results and those obtained by using the ASM is as good as it is for other deformation values. Such surprising behaviour has already been observed in other systems [6, 13, 16, 22], and can be easily understood here, at least qualitatively. In fact, when the trajectory crosses the separatrix and changes its topology, the particle is flying somewhere inside the cavity, between two successive bounces on the boundary. In other words, the crossing region is traversed diabatically rather than adiabatically, in almost any case. This separatrix crossing is studied numerically when the time evolution of the energy as well as that of the classical actions, is followed during the switching procedure [27].

As we have already seen for the quantum single-particle energy spectrum in a prolate cavity [18], all the spherical multiplets are split in the same way by the axial deformation. Some of these splittings are shown in figure 4. The energies change smoothly with deformation, the levels are simply ordered by increasing $|m|$. This

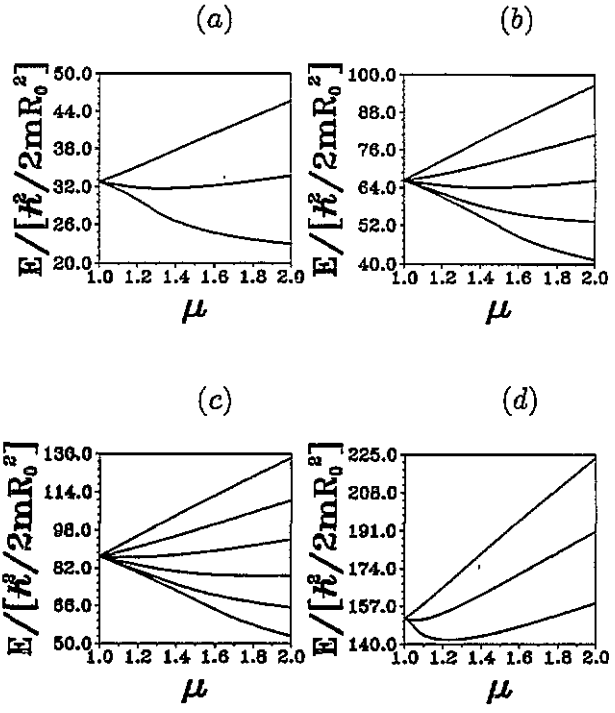

Figure 4. Examples of energy splittings in a prolate cavity, obtained by the ASM, for the $1d$ (a), $1g$ (b), $1h$ (c) and $3d$ (d) spherical multiplets. Each of these curves is obtained by averaging the classical energy of 25 trajectories.

behaviour is correctly predicted by perturbing trajectories using the classical perturbation theory with spherical symmetry. Indeed, let E_0 be the energy of a free particle inside a spherical cavity of radius R_0. Holding a constant volume and an axial symmetry along the z direction, let us give a small deformation $d\mu$ along the z axis of the cavity. The coordinates are now

$$\begin{aligned} x' &= x(1-\tfrac{1}{3}\,d\mu) \\ y' &= y(1-\tfrac{1}{3}\,d\mu) \\ z' &= z(1+\tfrac{2}{3}\,d\mu). \end{aligned} \tag{17}$$

The conjugate momenta are changed to

$$\begin{aligned} p'_x &= \frac{p_x}{1-\frac{1}{3}\,d\mu} \simeq p_x(1+\tfrac{1}{3}\,d\mu) \\ p'_y &= \frac{p_y}{1-\frac{1}{3}\,d\mu} \simeq p_y(1+\tfrac{1}{3}\,d\mu) \\ p'_z &= \frac{p_z}{1+\frac{2}{3}\,d\mu} \simeq p_z(1-\tfrac{2}{3}\,d\mu). \end{aligned} \tag{18}$$

Thus, the energy becomes, in spherical coordinates

$$E' = E_0[1-\tfrac{4}{3}P_2(\cos\theta)\,d\mu]. \tag{19}$$

In this equation we must average $P_2(\cos\theta)$ over all the possible orientations of the momentum $\boldsymbol{p}$. For the $L_z = 0$ levels, all the values of θ between 0 and 2π could be reached; therefore $\langle\cos^2\theta\rangle = \frac{1}{2}$.

For the $L_z \neq 0$ levels, the argument is more involved. Let the angular momentum $\boldsymbol{L}$ be in the plane yoz. The particle momentum $\boldsymbol{p}$ is evolving in a plane which is perpendicular to $\boldsymbol{L}$ and which makes an angle α with the z axis. The equation of this plane can be written in spherical coordinates as a function of L and L_z. The mean value $\langle\cos^2\theta\rangle$, calculated on the hodograph of the motion, takes the form, after a straightforward calculation

$$\langle\cos^2\theta\rangle = \frac{1}{2\pi}\,4u(1+u^2)^{1/2}\int_0^{\pi/2}\frac{\sin^2\phi}{(u^2+\sin^2\phi)^2}\,d\phi = \frac{1}{2(u^2+1)} \tag{20}$$

where

$$u = \cot\alpha = \frac{L_z/L}{(1-(L_z/L)^2)^{1/2}}. \tag{21}$$

The perturbed semiclassical energy is finally given by

$$E' = E_0\left(1+\frac{3L_z^2-L^2}{3L^2}\,d\mu\right) \tag{22}$$

a form similar to the quantum one where

$$\langle P_2(\cos\theta)\rangle_Q = -\frac{3m^2-l(l+1)}{(2l-1)(2l+3)} \tag{23}$$

for any $|nlm\rangle$ eigenstate. Therefore, the straight lines which are tangent to each single energy level, have slopes which range from:

$$\frac{E'-E_0}{E_0} \simeq -\tfrac{1}{3}\,\mathrm{d}\mu \qquad \text{for } L_z = 0 \text{ levels}$$

to

$$\frac{E'-E_0}{E_0} \simeq \tfrac{2}{3}\,\mathrm{d}\mu \qquad \text{for } L_z = L \text{ levels.}$$

Thus, for small axial deformations, semiclassical calculations are consistent with quantum ones. It must be noticed that the preceding result is quite general and can be applied to any axially deformed systems, Hamiltonian or not, and to any trajectories having the same starting energy for the spherical shape. Moreover, we can deduce from the preceding equations that the minimum energy is obtained for prolate ($\mu > 1$), oblate ($\mu < 1$) or spherical ($\mu = 1$) shapes respectively for $L_z < L/\sqrt{3}$, $L_z > L/\sqrt{3}$ and $L_z = L/\sqrt{3}$.

Figure 5 shows the complete single particle energy spectrum, up to an energy of $E = 250$ in units $\hbar^2/2mR_0^2$, in a prolate cavity, using the ASM, based on classical trajectories. For each level, 25 randomly chosen initial conditions are used to calculate the averaged energy, and the switching time T is fixed by requiring at least a thousand bounces on the boundary during the variation of the deformation. As the system remains integrable for any value of deformation, there are true crossings of the energy levels and no avoided crossing. This spectrum could be used as a basis for the study of the total energy of non-interacting Fermi-Dirac particles as a function of the deformation.

The single energy spectrum we will use is made of 323 single levels including the third $l = 9$ spherical multiplet. When the deformation increases, each spherical multiplet is split, as discussed above. Thus for each filling of the single levels we must be sure

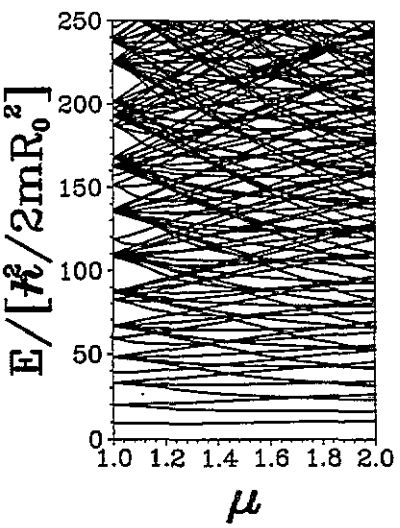

Figure 5. Single energy spectrum in a prolate cavity obtained by using the adiabatic switching method. All values of L_z are represented. This spectrum is similar to a Nilsson spectrum, without any spin orbit term, which is extensively used in nuclear physics.

that any level which is not yet included in our truncated basis does not come from high energy and is inserted among the lowest levels of the spectrum. These missing levels should have an angular quantum number, l, as high as possible, and $L_z = 0$. To avoid such a difficulty, we have included in the truncated basis the $L_z = 0$ level starting from the first $l = 15$ spherical multiplet, which is at an energy of $267.76\ \hbar^2/2mR_0^2$ for a deformation $\mu = 2$. The filling of this level should require considering 245 spinless particles for this value of the deformation, far beyond the number of particles we actually consider. Comparison of such a calculation with pure quantum prediction is done in the next section.

4. Total energy of N identical nucleons

The single particle energy spectrum, obtained by the ASM, may be used to study the total energy of an assembly of N non-interacting Fermi–Dirac spinless particles, as a function of the deformation, in a prolate cavity. For each value of the deformation, 323 basis levels are ordered by increasing energy, the lowest levels are then filled by one particle if the corresponding L_z value is zero and by two particles if L_z is different from zero, until the total number N is reached. This procedure defines a minimum energy configuration for a given value of the deformation. Of course, the filling of the levels could remain the same for a short range of deformation, but for each value of the deformation, the minimum energy configuration has to be found. Figure 6 shows the total energies for four different particle numbers. Each parabole-like curve is associated to one particular N-particle configuration which becomes the minimum energy configuration for some value of the deformation. Only the configurations having this property have been represented. The general shape of these curves was obtained long ago by Hill and Wheeler [36], for a rectangular box deformed at constant volume and filled by 60 spinless Fermi–Dirac particles. In order to obtain the ground state energy, in the deformation range under study, it is necessary to include only 10 different configurations for $N = 46$, but 36 different configurations for $N = 220$. In this latter case, the last filled level for a deformation $\mu = 2$ is at an energy around $250\hbar^2/2mR_0^2$. In this energy region, we are sure that there is no intruder single particle level which should come from higher energy and which is not yet included in our truncated basis.

The envelope of the semiclassical curves can be compared with quantum calculation using the asymptotic formula given by Balian and Bloch [31], for the average density of eigenvalues $\rho(k)$, inside a cavity with Dirichlet conditions on the boundary. If k is the wavenumber, V, S and K, respectively, the volume, the surface and the curvature of the cavity, then

$$\rho(k) = \frac{k^2 V}{2\pi^2} - \frac{kS}{8\pi} + \frac{K}{12\pi^2}. \tag{24}$$

For a cavity filled up to the Fermi level k_F by N non-interacting particles the total minimum energy is

$$E = \frac{\hbar^2}{2m}\frac{k_F^5 V}{10\pi^2}\left\{1 - \frac{5\pi}{16}\frac{S}{V}\frac{1}{k_F} + \frac{5}{18}\frac{K}{V}\frac{1}{k_F^2}\right\} \tag{25a}$$

with

$$N = \frac{k_F^3 V}{6\pi^2}\left\{1 - \frac{3\pi}{8}\frac{S}{V}\frac{1}{k_F} + \frac{1}{2}\frac{K}{V}\frac{1}{k_F^2}\right\}. \tag{25b}$$

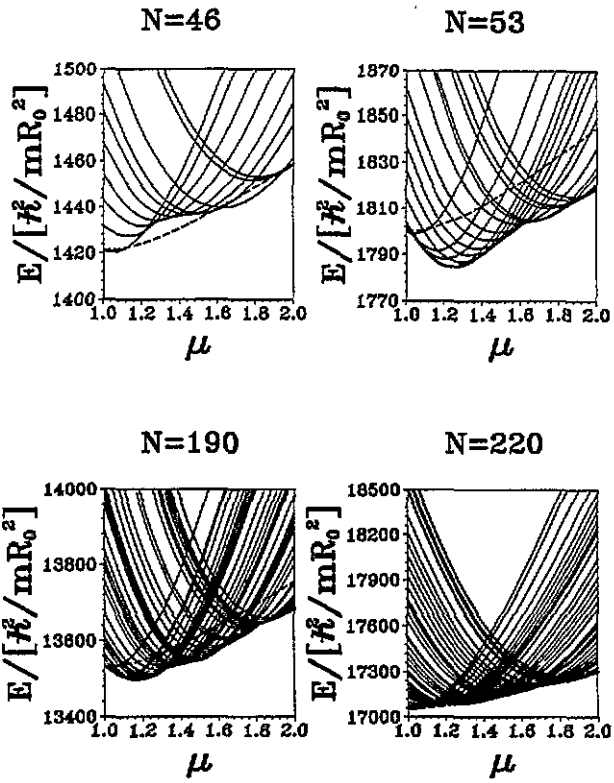

Figure 6. Total energy of N non-interacting Fermi–Dirac spinless particles in a prolate cavity as a function of the deformation μ. The dashed curve corresponds to a pure quantum calculation. For further details, see text.

A straightforward calculation gives the minimum energy E in units of $\hbar^2/mR_0^2$ as a series in powers of N:

$$E(N)=\frac{3}{10}\left(\frac{9\pi}{2}\right)^{2/3}N^{5/3}+\frac{9\pi}{32}\left(\frac{9\pi}{2}\right)^{1/3}N^{4/3}B_S+\left[\frac{27\pi^2}{128}B_S^2-B_K\right]N+\alpha N^{2/3}+\sigma(N^{1/3}) \tag{26}$$

where α is a constant not yet known analytically, B_S and B_K express the deviations from the sphere of the surface and the curvature terms of a prolate cavity [37]:

$$B_S=\frac{(1-e^2)^{1/3}}{2}\left\{1+\frac{\sin^{-1}e}{e(1-e^2)^{1/2}}\right\} \tag{27a}$$

$$B_K=\frac{1}{2(1-e^2)^{1/3}}\left\{1+\frac{1-e^2}{2e}\log\frac{1+e}{1-e}\right\} \tag{27b}$$

with $e^2=1-\mu^{-2}$.

The smooth average total energy given by equation (34) is represented in figure 6 by a dashed line, for each particle number. The absolute position of the curve is fixed by the total semiclassical energy for the spherical cavity, and therefore the unknown constant α, in (34), is determined by the exact semiclassical energy. The corresponding quantum energy would be, in any case, larger than the preceding one, the relative difference would be a few per cent. The semiclassical ground state energy, which is

given by the envelope of all the parabole-like curves, has the same global trend as the pure quantum calculation when the deformation increases. The best agreement between the two different approaches is obtained for $N=220$, where the quantum minimal energy merges into the semiclassical envelope. Nevertheless, for the other particle numbers shown in figure 6, some deviations between the two calculations must be explained. In fact, these deviations are easily understood by looking at shell effects which occur by filling the single levels of the energy spectrum shown in figure 5. Let us consider, for example, the case with 46 particles. Starting from the spherical cavity, the latest occupied level is the $3s$ singlet, the energy of which is around 90 in the proper unit used in figure 5, and the lowest unoccupied levels are the $2f$–$1i$ multiplets around an energy of $110\hbar^2/2mR_0^2$. Thus, $N=46$ corresponds to the closure of a spherical shell and the minimal configuration remains the same when the deformation increases until a value $\mu \approx 1.2$ (see figure 5). For a larger deformation, the $L_z=0$ level starting from the $2f$ spherical multiplet crosses one of the levels already occupied and thus the minimal configuration is changed as well as the ground state energy. For higher deformations, the splittings of the $2f$–$1i$ multiplets induce other crossings of the single particle levels and the minimal configuration is changed as the deformation increases. For $N=46$, the closure of the spherical shell corresponding to the filling of the $3s$ singlet leads to an equilibrium shape which does not have exact spherical symmetry, but a small prolate shape around $\mu \approx 1.05$. The closure of the spherical shell is clearly underlined by the appearance of a bump on the semiclassical envelope between $\mu \approx 1.2$ and $\mu \approx 1.6$. For $N=53$, the behaviour is different, as shown in figure 6; here, we choose a particle number which corresponds to the following filling in the spherical cavity: the $2f$ multiplet is fully occupied, but almost at the same energy lies the $1i$ multiplet which is unoccupied (see figure 5). This case corresponds to an open shell which is closed for $N=69$ by filling all the single levels in a spherical cavity up to an energy of $120\hbar^2/2mR_0^2$. Therefore, for a small prolate deformation, the splitting of the $1i$ multiplet, according to the results obtained in the previous section, mixes all its levels with those coming from the $2f$ multiplet. This splitting and mixing allows the system to find, for a small deformation, a lowest ground state configuration by filling the levels coming from the $1i$ multiplet. This fast change in the filling over a small deformation range explains why the equilibrium shape is obtained for a prolate deformation around $\mu \approx 1.23$. The same discussion can be had for $N=190$ which corresponds also to an open shell between the shell closures at $N=169$ and $N=199$, corresponding to the single particle energies around 200 and 225, respectively, in the energy unit used in figure 5. The final case shown in figure 6, i.e. $N=220$, corresponds to the filling of all the energy levels under $250\hbar^2/2mR_0^2$, in spherical symmetry, and is quite similar to $N=46$, but with many more minimal configurations which obliterate almost all the shell effects. The semiclassical analysis of the shell effects and the oblate–prolate asymmetry in nuclei was carefully analysed by H Frisk [38] by using the periodic orbit theory of Gutzwiller [39]. In this work, it was shown that the lengths of the most important periodic orbits remain almost constant in a spheroidal oblate cavity although these lengths vary for a prolate deformation. Consequently, an energy minimum region arises for a prolate deformation around $\mu=1.3$, which is also seen in our approach, for almost any number of particles.

Now, if we consider an oscillating boundary around a fixed deformation, the curves presented in figure 6 allow us to calculate the dissipation energy rate of the system. Indeed, if the particles do not have the necessary time to minimize their total energy during the oscillation, they remain in the same configuration and the dissipation energy

is estimated by the corresponding parabole-like curves. On the contrary, if the oscillation is adiabatic, then the dissipation rate is given by the smooth envelope.

5. Conclusion

We have shown in this paper that the ASM is able to reproduce, within a good approximation, the variation of the energy levels of a prolate cavity with deformation. It is important to note that quantum mechanics (or wave mechanics since the problem of the eigenmodes of the cavity occurs also outside the frame of quantum mechanics) determines the values of the actions I_ε and I_ξ and the eigenspectrum only for $\mu = 0$. The behaviour of the energy levels as a function of μ is, however, determined only by classical mechanics during the adiabatic switching of the deformation. Table 1 shows that the ASM is a very good approximation when compared with the exact calculation. Therefore the shell effects which arise when summing up the energy levels as in figure 6 are indeed effects which do result from the classical evolution with deformation. The formula given by Balian and Bloch erase those effects as we have clearly shown here.

The variation of the spectrum with a parameter adiabatically switched has been calculated previously in other cases, for example in [6, 7] for the case of a Henon-Heiles-like system or for the case of the Hecht Hamiltonian [10]. In none of these cases is the usefulness of the method to build up shell effects detected. For further details on the method one should read the review by W P Reinhardt [40]; another paper [27] provides more details about conservation of the actions and the resonances.

Acknowledgment

One of us (FB) is very grateful to Dr W J Swiatecki for many enlightening discussions during this work. He would like also to acknowledge the Lawrence Berkeley Laboratory hospitality where part of this work was done, and where the good working conditions and fruitful discussions in the nuclear theory group were greatly appreciated.

References

[1] Einstein A 1917 *Verh. Dtsch Phys. Ges.* **19** 82
Brillouin L 1926 *J. Physique* **7** 353
Keller J B 1958 *Ann. Phys.* **4** 180
[2] Percival I C 1977 *Adv. Chem. Phys.* **36** 1
Noid D W, Koszykowski M L and Marcus R A 1981 *Ann. Rev. Phys. Chem.* **32** 267
de Leon N and Heller E J 1983 *J. Chem. Phys.* **78** 4005
Miller W H 1984 *J. Chem. Phys.* **81** 3573
Martens C C and Ezra G S 1985 *J. Chem. Phys.* **83** 2990; 1987 *J. Chem. Phys.* **86** 279
[3] Ehrenfest P 1916 *Versl. Kon. Akad. Amsterdam* **25** 412 [Engl. transl. 1967 *Sources of Quantum Mechanics* ed B L Van der Waerden (New York: Dover)]
[4] Solov'ev E A 1978 *Zh. Eksp. Teor. Fiz.* **75** 1261 [*Sov. Phys.-JETP* **48** 635]
[5] Grozdanov T P and Solov'ev E A 1982 *J. Phys. B: At. Mol. Phys.* **15** 1195
[6] Skodje R T, Borondo F and Reinhardt W P 1985 *J. Chem. Phys.* **82** 4611
[7] Johnson B R 1985 *J. Chem. Phys.* **83** 1204
[8] Carbonell J, Brut F, Arvieu R and Touchard J 1985 *J. Phys.* G **11** 325
[9] Skodje R T and Borondo F 1985 *Chem. Phys. Lett.* **118** 409
[10] Patterson C W 1985 *J. Chem. Phys.* **83** 4618

[11] Grozdanov T P, Saini S and Taylor H S 1986 *Phys. Rev.* A **33** 55
[12] Skodje R T and Borondo F 1986 *J. Chem. Phys.* **84** 1533
[13] Grozdanov T P, Saini S and Taylor H S 1986 *J. Chem. Phys.* **84** 3243
[14] Skodje R T and Borondo F 1986 *J. Chem. Phys.* **85** 2760
[15] Jaffé C 1986 *J. Chem. Phys.* **85** 2885
[16] Patterson C W, Smith R S and Shirts R B 1986 *J. Chem. Phys.* **85** 7241
[17] Johnson B R 1987 *J. Chem. Phys.* **86** 1445
[18] Arvieu R, Brut F, Carbonell J and Touchard J 1987 *Phys. Rev.* A **35** 2389
[19] Reinhardt W P and Dana I 1987 *Proc. R. Soc.* A **413** 157
[20] Dana I and Reinhardt W P 1987 *Physica* **28** 115
[21] Saini S and Farelly D 1987 *Phys. Rev.* A **36** 3556
[22] Zakrzewski J, Saini S and Taylor H S 1988 *Phys. Rev.* A **38** 3877, 3900
[23] Scharf R 1988 *J. Phys. A: Math. Gen.* **21** 4133
[24] Jaffé C and Watanabe M 1988 *J. Chem. Phys.* **89** 6329
[25] Martens C C, Waterland R L and Reinhardt W P 1989 *J. Chem. Phys.* **90** 2328
[26] Billing G D and Jolicard G 1989 *Chem. Phys. Lett.* **155** 521
[27] Brut F 1993 *J. Phys. A: Math. Gen.* **26** 4767
[28] Moszkowski S A 1955 *Phys. Rev.* **99** 803
Nilsson S G 1955 *Mat. Fys. Medd. Dan. Vid. Selsk.* **29**(16)
Bohr A and Mottelson B R 1975 *Nuclear Structure* vol II (Reading, MA: Benjamin)
[29] Gignoux C and Brut F 1989 *Amer. J. Phys.* **57** 422
[30] Carbonell J, Brut F, Arvieu R and Touchard J 1984 *J. Physique* **45** C6-351
[31] Balian R and Bloch C 1970 *Ann. Phys.* **60** 401
[32] Strutinsky V M 1974 *Proc. 7th Masurian School in Nucl. Phys., Mikolajki, Poland, September* (1975 *Nucleonica* **20** 679)
Strutinsky V M and Magner A G 1976 *Elementary Particles and Nuclei* 7 356
Strutinsky V M, Magner A G, Ofengenden S R and Dossing T 1977 *Z. Phys.* A **283** 269
[33] Ayant Y and Arvieu R 1987 *J. Phys. A: Math. Gen.* **20** 397
[34] Arvieu R and Ayant Y 1987 *J. Phys. A: Math. Gen.* **20** 1115
[35] Keller J B and Rubinov S I 1960 *Ann. Phys.* **9** 24
[36] Hill D L and Wheeler J A 1953 *Phys. Rev.* **89** 1102
[37] Hasse R W and Myers W D 1988 *Geometrical Relationships of Macroscopic Nuclear Physics* (Berlin: Springer)
[38] Frisk H 1990 *Nucl. Phys.* A **511** 309
[39] Gutzwiller M C 1967 *J. Math. Phys.* **8** 1979; 1969 *J. Math. Phys.* **10** 1004; 1970 *J. Math. Phys.* **11** 1791
Gutzwiller M C 1991 *Chaos and Quantum Physics (Les Houches, session LII, August 1989)*, ed M J Giannoni, A Voros and J Zinn-Justin (Amsterdam: North-Holland) p 201
[40] Reinhardt W P 1989 *Adv. Chem. Phys.* **73** 925